5A.7 A CONICAL SCAN TYPE SPACEBORNE PRECIPITATION RADAR

Ken'ichi Okamoto*[1], Shoichi Shige[2] , and Takeshi Manabe[3]

1: Tottori University of Environmental Studies, Tottori, Japan

2: Kyoto University, Kyoto, Japan

3: Osaka Prefecture University, Sakai, Japan

1. INTRODUCTION

The global distribution of rainfall and its variation are deeply linked to the global climate change and the abnormal weather and they have significant impacts on the human activities and social systems. In order to acquire global rainfall data, we have to rely on observations by the spaceborne rain radar or microwave radiometer. The TRMM satellite , which was launched on 28 November 1997, realized the first spaceborne rain radar called the TRMM PR(Kozu et al. 2001). TRMM PR has been acquiring many valuable three dimensional distribution data of rainfall, which cannot be observed by other methods, for more than eleven years and ten months.

However, as the TRMM PR adopts an active phased array system composed of as many as 128 transmitting and receiving elements to scan antenna beam electrically at high speed, TRMM PR has the extremely heavy weight*(465 kg*), which is not always desirable for the spaceborne system. In addition, TRMM PR's single wave guide slot array antenna cannot be shared by the multi-frequency and dual polarization radar, meaning that each different frequency and polarization radar needs different slot array antenna. Therefore from a physical size and weight point of view, using multiple slot array antennas for the future multi-frequency and dual polarization radar, is not preferable.

* *Corresponding author address:* Ken'ichi Okamoto, Tottori University of Environmental Studies, Tottori 689-1111, Japan; e-mail: kokamoto@kankyo-u.ac.jp

This study aims at designing of the small and light rain radar system which utilizes the high speed mechanical scan reflector antenna, doing simulation of the rain observation from space by using the cloud resolving model, and assessing of the design specification of the new spaceborne conical scanning type rain radar. We study the single frequency and polarization conical scan type rain radar which becomes the basis of the future multi-parameter rain radar system. The conical scan is widely used in the spaceborne microwave radiometer, such as the AMSR-E on the Aqua satellite(Kawanishi et al. 2003). If the small and light spaceborne rain radar that can be installed on the many satellites is proposed, opportunities of rain observations from space will increase, which will lead to more accurate observations of global rainfall distributions and its variations. That will surely bring significant contributions to studies of the global climate change and abnormal weather.

2. CALCULATIONS OF SYSTEM PARAMETERS

We calculate system parameters of the satelliteborne conical scan type rain radar, varying the antenna diameter D and the scan angle of conical scan (=cone angle) η as two variable parameters. Fig. 1 shows the concept of the conical scan. The antenna beam is scanned conically around the z-axis which points to the nadir direction. The scan angle η is the same as the cone angle, and H is the satellite altitude. The antenna beam width and the angular

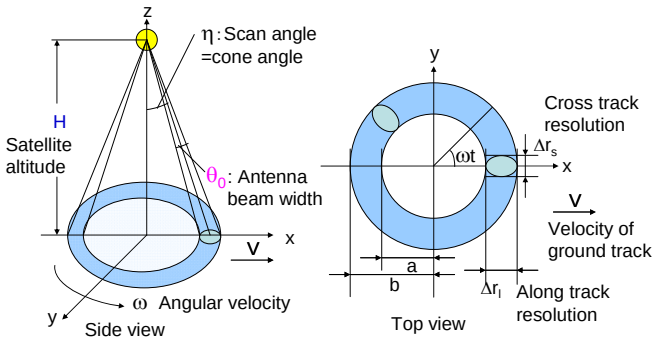

Fig. 1. Concept of the conical scan.

velocity of the conical scan are given by θ_0 and ω, respectively. In order to observe a raining area without making any gaps between adjacent swaths, a satellite must move the same distance as the along track resolution Δr_l while the antenna beam goes round a circle with the period T. This condition means $T= \Delta r_l /v$, where v is the velocity of the ground track of the satellite. The angular velocity ω is given by $\omega = 2\pi/T = 2\pi v/\Delta r_l$. The along track resolution Δr_l and the cross track resolution Δr_s are given by $\Delta r_l = H\theta_0/\cos^2\eta$, and $\Delta r_s = H\theta_0/\cos\eta$, respectively. The $2a$ and $2b$ mean internal and external diameters of the scan circle. We assume that the satellite altitude H is equal to the altitude of the GPM satellite $H=407$ *km*, which mounts dual frequency precipitation radar (DPR) and is scheduled to be launched in 2013. The rain radar frequency f and the pulse width τ are assumed equal to these of the Ku-band radar of DPR, $f=13.6$ *GHz*, and $\tau=1.67\mu s$.

The direction which antenna beam points is called as the angle-bin direction. The rain scattered received power from an angle-bin direction must be averaged by the independent sample number $2N_d$ to suppress fluctuations of the received power. The $2N_d$ takes *64* in the TRMM PR by applying the two frequency agility technique. This means 32 pairs of pluses are transmitted to an angle-bin direction. Pulses in a pair have slightly different frequencies. In order to ensure more than 32 independent pulse pairs, the *PRF* must be large enough. Therefore, *PRF* is determined from the condition that the rain echo of the first transmitted pulse is received between the *n*-th and *(n+1)*-th transmitted pulse. In the determination of *PRF*, the margin time T_m for the transmit-receive switching must be larger than *10* μs. Also the margin time for the satellite altitude variation ΔH and the antenna pointing error must be considered to determine *PRF*. The angle-bin number per a single revolution N_a is determined by $N_a = 2\pi(a+\Delta r_l/2)/\Delta r_s$. The dwell time of an antenna beam in an angle-bin direction T_a is determined from $T_a = T/N_a$, where T is the period of a single revolution. The independent pulse pair number N_d is determined from $N_d = PRF \times T_a$ and the independent sample number becomes $2N_d$.

S_{min}: Minimum detectable power

$$S_{min} = N_F k_B T_e B$$

N_F: Receiver noise figure(=3.0 dB)
k_B : Boltzmann constant (=1.38065 × 10^{-23} J/K)
T_e:Ambient temperature(=290 K)
B : Receiver band width(=0.78 MHz)
S_{min} = -112.05 dBm

Radar equation

$$P_r = \alpha \frac{P_t G_0^2 (C\tau)\theta_0^2 \pi^3}{2^{10}(\ln 2) r_t^2 \lambda^2 L} \left|\frac{\varepsilon - 1}{\varepsilon + 2}\right|^2 Z_e \exp(-0.2 \cdot \int_0^{H_B/\cos\eta} k dr \cdot \ln 10)$$

P_t :Transmitted peak power
P_r :Received power
C :Velocity of light
τ: Pulse width(=1.67 μs)
L : System loss(=2.4 dB)
ε:Complex permittivity of water
α:Transmit-receive beam overlap rate
H_B : Thickness of bright band (=0.5 km)
H_{ru} : Thickness of uniform rain layer (=5 km)

$|(\varepsilon - 1)/(\varepsilon + 2)|^2 = 0.9255$
λ: Wavelength(=2.204 cm)
Distance between satellite and rain top $r_t = (H - H_{ru})/\cos\eta$
G_0 :Antenna Gain
θ_0:Antenan beam width

Z-R relation $Z_e = 234R^{1.59}$
k-R relation $k = 0.0237R^{1.17}$

Fig. 2. Radar equation

The transmitted peak power P_t required to observe the minimum detectable rain rate R *(=1 mm/h)* at the rain top is calculated from the radar equation shown in the Fig. 2. The uniform rain model which has the height H_{ru} of *5 km* and the rain rate of *1 mm/h* is assumed. The bright band which has the thickness H_B of *0.5 km* above the rain layer is also assumed. Meanings of the symbols used in the radar equation are also shown in the Fig. 2. The symbol α means the transmitted-received beam overlap rate, because antenna pointing directions of

the transmitting and the receiving slightly differ by the continuous conical scanning. The relations between the radar reflectivity factor Z_e *(mm^6/m^3)*, the attenuation coefficient *k (dB/km)* and the rain rate *R (mm/h)* are assumed $Z_e=234R^{1.59}$, and $k=0.0237R^{1.17}$, respectively assuming the Marshall-Palmer (Marshall and Palmer 1948)rain drop size distribution. Putting, the received power P_r equals to the minimum detectable power S_{min}, the required P_t is determined. The parameters of the conical scan radar is summarized in the Table 1 when the antenna Diameter *D=1 m*, and the scan angle η*= 11 deg.*

Table 1 An example of the conical scan radar parameter (*D=1 m*, η*=11 deg*.).

Conditions precedent	
Frequency f [GHz]	13.6
Antenna diameter D [m]	1.0
Scan angle η [deg]	11
Range resolution $c\tau/2$ [m]	250
System loss L [dB]	2.4
Receiver noise figure N_F [dB]	3.0
Ambient temperature T_e [km]	290
Receiver band width B [MHz]	0.78
Thickness of bright band H_B [km]	0.5
Height of rain layer H_{ru} [km]	5
Satellite altitude H [km]	407
Variation of satellite ΔH [km]	11
Maximum height of rain H_r [km]	15
Minimum detectable rain rate R [mm/h]	1.0
Velocity of ground track V [km/s]	7.205

Determined parameters	
Items	Values
Antenna beam width θ_0 [deg]	1.459
Along track resolution Δr_l [km]	10.76
Cross track resolution Δr_s [km]	10.57
Scan width(internal) 2a [km]	147. 50
Scan width(External) 2b [km]	169.01
Scan period T [s]	1.493
Angular velocity ω[deg/ s]	241.13
Antenna gain G_0 [dB]	42.17
S_{min} [dBm]	- 112.05
Beam overlap rate	0.89
Transmitted peak power P_t [W]	1205. 2
Angle- bin number N_a	48
n	4
PRF	1289
Independent sample number N_d x 2	80

The independent sample number $2N_d$, and the transmitted peak power P_t are calculated for the antenna diameter *D=0.8, 1, 1.4, 1.6, and 1.8 m* and for the scan angle η*=5, 8, 11, 14, 17, 20, 23, 26, and 29 deg.* These values are shown in the Fig. 3, and Fig. 4, respectively. However, when the geometric optics reflected wave by the main reflector is blocked by the primary horn, the calculations were not made. These situations happen when η*=5 deg. (for D=1, 1.4, 1.6, and 1.8 m)* and η*=8 deg. (for D=1.6, and 1.8 m)*. The independent sample number of more than 64 cannot be attained when *D=1.4 m* (for η*=26*, and *29 deg.)* , *D=1.6 m* (for η*=20, 23, 26*, and *29 deg.*), and D=1.8 m(for η*=17, 20, 23, 26*, and *29 deg.*). When

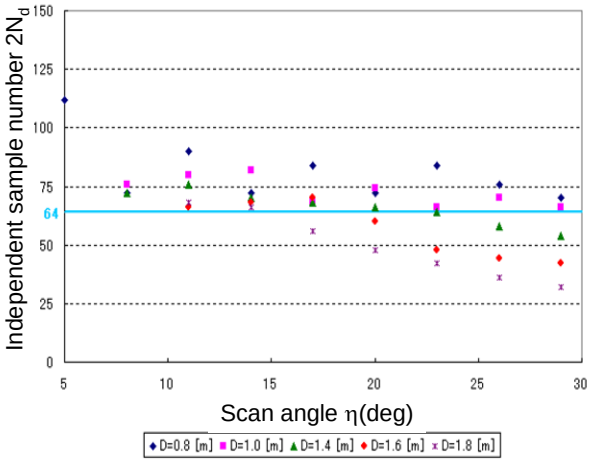

Fig. 3. Independent sample number $2N_d$ as a function of the scan angle η, where the antenna diameter *D* is the variable parameter.

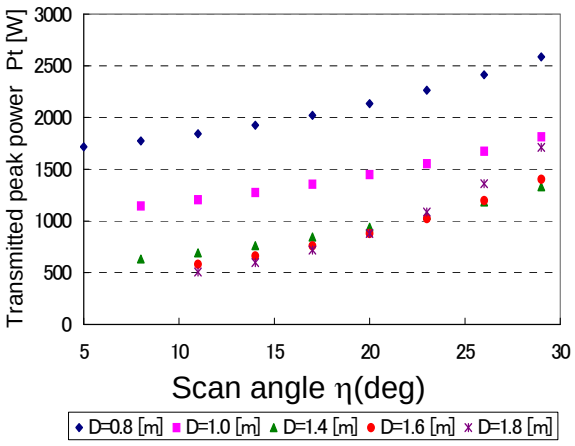

Fig. 4. Transmitted peak power P_t*(W)*as a function of the scan angle η, where the antenna diameter *D* is the variable parameter.

the antenna diameter *D* is fixed, the required transmitted peak power increases as the scan angle increases. When the scan angle η is narrow, the required transmitted peak power increases as the antenna diameter decreases. At the same time, this is not applicable when the scan angle is wide. This is because the transmitted-received beam overlap rate α decreases as the *D* and η increases .

3. SIMULATIONS OF RAIN OBERVATION

We run an experimental simulation on the rain observation from space by the conical scan radar, varying the antenna diameter *D* and the scan angle η as two variable parameters. The simulation was performed for antenna diameters *D* of *0.8, 1, 1.4, 1.6, and 1.8 m*, increasing scan angles η from 5 deg. to 29 deg. by 3 deg. The radar reflectivity factor $Z_{e\text{-}r}$, for which rain attenuation correction is performed, is calculated for the center point of the rain scattering volume . The cloud resolving model is used to give the true value of the radar reflectivity factor Z_e at the same center point of the rain scattering volume. Finally, correlation coefficients between the calculated radar reflectivity factor $Z_{e\text{-}r}$ and true Z_e of every center point of the rain scattering volume, which the conical scan radar observes, are calculated to estimate the accuracy of the observation.

3.1 Rain Model

We used the Goddard Cumulus Ensemble (GCE) model (Tao and Simpson 1993). This model has 256 grid points x 256 grid points in the horizontal direction. As the horizontal resolution is *2 km*, the area is *510 km x 510 km*. The model has 80 grid points in the vertical direction with the vertical resolution of *0.25 km* and the vertical height is *19.75 km*. The radar reflectivity factor Z_e is calculated for every unit cell in the three dimensional lattice. The rain rate *R* is calculated from the mixing ratio of rain, snow, hail and their fall velocity in the beginning. Then, the radar reflectivity factor Z_e is calculated by Z_e-*R* relation $Z_e=234R^{1.59}$, which is calculated from the raindrop size distribution by Marshall-Palmer. This Z_e value is treated as the true value for the simulation.

Fig. 5 shows examples of trajectories of the conical scan superimposed on the cloud resolving model, when *D=0.8 m, η= 5 deg*. and when *D=1.8 m, η= 29 deg*. The abscissa shows the along-track direction, and the ordinate shows the antenna swath width which depends on the antenna diameter *D* and the scan angle η.

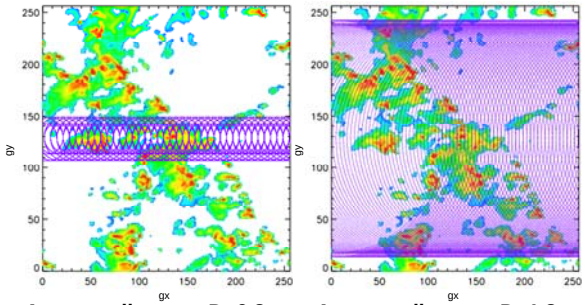

Antenna diameter D=0.8 m , Scan angle η=5 deg. **Antenna diameter D=1.8 m , Scan angle η=29 deg.**

Fig. 5. Trajectory of the conical scan superimposed on the cloud resolving model.

3.2 Antenna Pattern

The primary horn points to the zenith direction, and the main reflector of the offset parabolic antenna is scanned conically around the axis which points to the nadir direction. The antenna pattern of the offset parabolic antenna is calculated. The offset angle is set to be equal to the scan angle, the phase center of the primary horn is placed at the focal point of the antenna. The edge level of radiation at the main reflector by the primary horn is *-11 dB*. The focal length of the antenna is set to be *5 m* to avoid the blocking of the main beam by the satellite body. The effect of the blocking and diffraction by the satellite body and the supporting constructions of the main reflector are neglected. The reflection by the main reflector is treated by the physical optics. The far field radiation pattern is calculated by the antenna analysis software GRASP8 of the TICRA Co., Ltd. (Pontoppidan 2003) for antenna diameters *D* of *0.8, 1, 1.4, 1.6, and 1.8 m*, increasing scan angles η from 5 deg. to 29 deg. by 3 deg.

An example of the far- field radiation pattern is shown by the blue curve in the left panel of the Fig. 6,

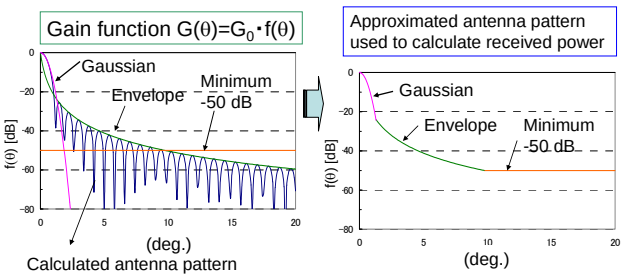

Fig. 6. Antenna pattern and its approximation (Scan angle η=*17 deg.* , Antenna diameter *D=1.6 m*).

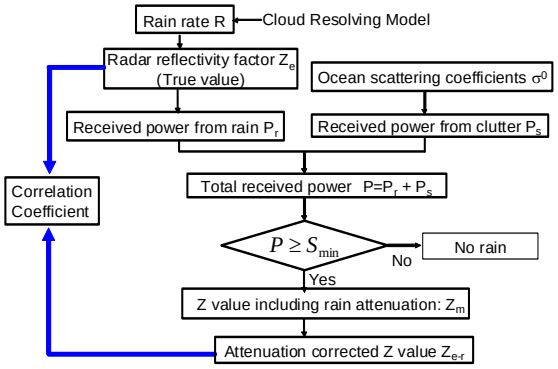

Fig. 7. Simulation flow of the rain observation by radar.

where the antenna pattern is assumed to be axially-symmetrical to the beam center and only the right-hand part is shown for the antenna diameter *D=1.6 m* and the scan angle η*=17 deg*. In the actual calculation, the envelope curve of the antenna pattern shown by the green curve is approximated by the least square method and is used to consider seriously the effect of the sidelobe area. The mainlobe area is approximated by the Gaussian pattern shown by the pink curve. It is difficult to the keep the sidelobe level less than some certain level in the actual antenna pattern for the far angle area from the beam center. Therefore, the minimum of the sidelobe level is assumed to take -50 dB shown by the brown line. The approximated antenna pattern used in the simulation is shown in the right panel of the Fig. 6.

3.3 Simulation flow

We show the simulation flow of rain observation by Fig. 7. As the radar receives simultaneously the rain scattered power P_r and ocean surface clutter power P_s which come from the same distance from the radar, the total received power becomes $P=P_r+P_s$. If P is larger than the minimum detectable power S_{min}, Z_m , which is affected by the rain attenuation, is calculated from P by using the radar equation. The rain attenuation correction is made by the Hitchfeld Bordan(Hitschfeld and Bordan 1954) method using the *k-Z* relation which is based on the Marshall-Palmer raindrop size distribution, and the radar reflectivity factor $Z_{e\text{-}r}$ after the rain attenuation correction is obtained. These calculations are made for the every center point of the rain scattering volume defined by the angle-bin(antenna beam width θ_0)and the range-bin(pulse width τ) . The cloud resolving model is used to give the true radar reflectivity value Z_e at the every center point of the rain scattering volume. The Z_e value of the unit cell in which the center point of the rain scattering volume belongs becomes the true Z_e value. Finally, correlation coefficients between the calculated radar reflectivity factor $Z_{e\text{-}r}$ and the true Z_e of the every center point of the rain scattering volume which the conical scan radar observes are calculated to estimate the accuracy of the observation.

Fig. 8 shows the calculation of the rain scattered received power P_r at the center points of the rain scattering volumes such as the number 1, 2, 3…shown in the left panel of the Fig. 8. Most of the rain scattered power comes from the rain scattering volume defined by the antenna beam width θ_0 and range-bin length of $c\tau/2$(*=250 m*). However, the rain echoes in the wide sidelobe area which comes from same distances from the radar are also received simultaneously with the rain echoes in the mainlobe rain scattering volume. Therefore P_r at the center

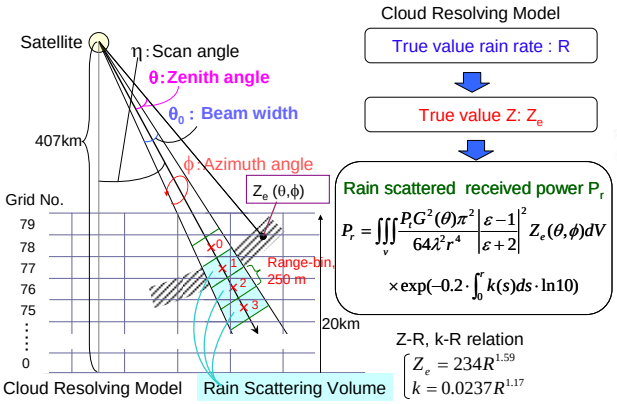

Fig. 8. Calculation of the rain scattered received power.

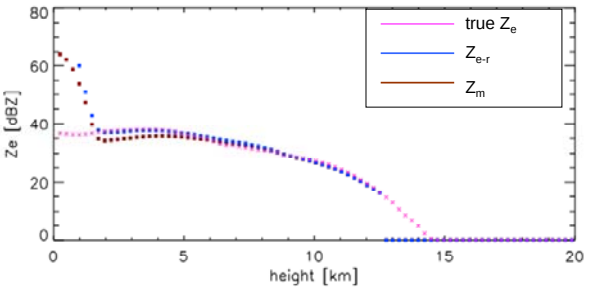

Fig. 9. An example of the true radar reflectivity factor Z_e and simulated radar reflectivity factors $Z_{e\text{-}r}$, Z_m vs. height. (Cloud Resolving Model, D=1.4m, η=11 deg.)

points of the rain scattering volumes is calculated by the integration of function including $G(\theta)^2 \times Ze(\theta, \phi)$ which is shown in Fig. 8.

We used ocean surface scattering coefficients σ^0 data obtained from *14. 6 GHz* SEASAT scatterometer by Wentz (Wentz et al. 1984) in the calculation of ocean surface clutter power. We used σ^0 data at the wind speed of 8.14 m/s and at the up-wind direction. We calculated the signal to clutter ratio(*S/C*), where *S* value was taken to be equal to S_{min} . We used only the $Z_{e\text{-}r}$ in the area where the S/C is larger than 10 dB in the calculation of correlation coefficients.

3.4 Simulation results

An example of the true radar reflectivity factor Z_e and simulated radar reflectivity factors $Z_{e\text{-}f}$ and Z_m as a function of height are shown in Fig. 9, where the antenna diameter *D=1.4 m* and the scan angle *η=11 deg*. The pink curve shows the true Z_e, the brown curve shows Z_m including rain attenuation and the blue curve shows $Z_{e\text{-}r}$ after the rain attenuation correction. As there is no rain above the height of 15 km, both Z_e and $Z_{e\text{-}r}$ give *0* dBZ. Although it rains slightly from the height of 12.5km to the height of 15 km, the radar cannot receive the echo which is below the minimum detectable power. The true Z_e and the simulated $Z_{e\text{-}r}$ agree well from the height of 6 km to the height of 12. 5 km. Although Z_m is smaller than Z_e by the effect of rain attenuation from the height of 1. 5 km to 6 km, $Z_{e\text{-}r}$ and Z_e agree well in the same area. The effect of the ocean surface clutter increases below the height of 1.5 km.

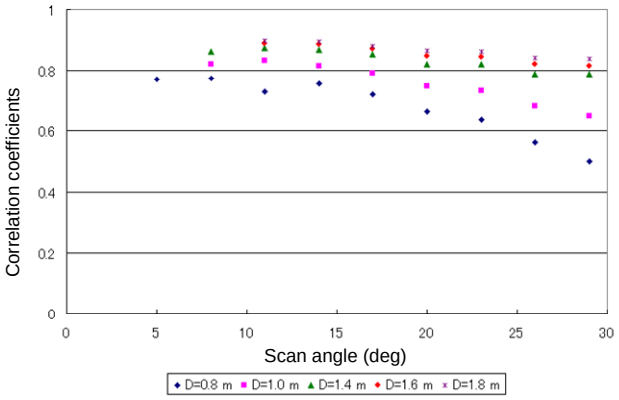

Fig. 10. Correlation coefficients between the true Z_e and the calculated $Z_{e\text{-}r}$.

Correlation coefficients between Z_e and $Z_{e\text{-}r}$ are shown in the Fig. 10. The abscissa shows the scan angle η, and the ordinate shows the correlation coefficients, where the antenna diameter *D* is used as

a parameter. The correlation coefficient decreases as the scan angle increases because the vertical resolution of the rain scattering volume increases rapidly as the scan angle increases. As the rain rate distribution varies more significantly by the vertical height than by the horizontal distance, the increase of the vertical resolution results large disagreement with the true value. The correlation coefficient increases as the antenna diameter increases because the rain scattering volume decreases and effects of rain which are outside from the antenna beam center decrease. When the scan angle is small, the variation of the correlation coefficient with the antenna diameter is small. However, the variation of the correlation coefficient with the antenna diameter increases as the scan angle increases. This is also because the vertical resolution of the rain scattering volume increases rapidly as the scan angle increases and the antenna diameter decreases.

4. SUMMARY OF SYSTEM PARAMETERS

Table 2 Examples of system parameters of the conical scan rain radar

	Radar #1	Radar # 2	TRMM PR
Antenna diameter D [m]	1.0	1.4	2.1
Scan angle η [deg]	11	11	17
Satellite altitude H [km]	407	407	350
Pulse width τ[μs]	1.67×2	1.67×2	1.67×2
Antenna beam width θ_0 [deg]	1.46	1.04	0.71
Along track resolution Δr_l [km]	10.76	7.71	4.3
Swath width（External）2b [km]	169.01	165.95	215
PRF [Hz]	1290	2396	2773
Independent sample number N_d	80	76	64
Antenna gain G_0 [dB]	42.2	45.1	47.7
S_{min} [dBm]	-112.05	-112.05	-112.6
Transmitted peak power P_t [W]	1205.19	691.68	572.1
Weight W [kg]	89	112	465
Power consumption P [W]	98	198	213

We propose the system parameters of the spaceborne small and light new conical scanning type rain radar. We summarize system parameters in Table 2 for the antenna diameter *D=1 m*, the scan angle η*=11 deg*., and for the antenna diameter *D=1.4 m*, the scan angle η*=11 deg*. The estimated weights are 89 kg for *D=1 m*, and 112 kg for *D=1.4 m*. These weights are much smaller than TRMM PR's weight of 465 kg.

5. CONCLUSION

Calculations of system parameters of the satelliteborne conical scan type rain radar were performed, where the antenna diameter *D* and the scan angle (=cone angle) η are two variable parameters.

Simulations of the rain observation by the conical scan type rain radar were performed, where the offset parabolic antenna pattern and the cloud resolving model are used.

Calculations of correlation coefficients between the true Z_e values and simulated $Z_{e\text{-}r}$ values were performed. Even if the antenna diameter is small, correlation coefficients are large when the scan angle is small.

System studies of the spaceborne conical scan type radar including estimation of the weight and the power consumption were performed. Estimated weights of the conical scan type rain radar become much smaller than TRMM precipitation radar.

From these results, it is concluded that the small and light spaceborne conical scan type precipitation radar is feasible.

Acknowledgments.

This research was supported by "Ground-based Research Program for Space Utilization" promoted by Japan Science Forum.

References

Kozu T., T. Kawanishi, H. Kuroiwa, M. Kojima, K. Oikawa, H. Kumagai, K. Okamoto, M. Okumura, H. Nakatsuka, and K. Nishikawa, 2001:

Development of Precipitation Radar Onboard the Tropical Rainfall Measuring Mission (TRMM) Satellites, IEEE Transactions on Geoscience and Remote Sensing, 39(1), 102-116.

Kawanishi, T. , T. Sezai, Y. Ito, K. Imaoka, T. Takeshima, Y. Ishido, A. Shibata, M. Miura, H. Inahata, and R. W. Spencer, 2003: The Advanced Microwave Scanning Radiometer for the Earth Observing System (AMSR-E), NASDA's Contribution to the EOS for Global Energy and Water Cycle Studies, IEEE Transactions on Geoscience and Remote Sensing, 41(2), 184-194.

Tao, W.-K., and J. Simpson, 1993: Goddard cumulus ensemble model. Part I: Model Description, Terrestrial Atmospheric and Oceanic Sciences., 4, 35-72.

Marshall J.S. and W.M. Palmer, 1948 : The distribution of raindrops with size, J. Meteorol., 5, 165-166.

Pontoppidan K. (Ed.), 2003: Technical Description of GRASP8, TICRA, Copenhagen, Denmark.

Hitschfeld W. and J. Bordan, 1954 : Errors inherent in the radar measurement of rainfall at attenuating wavelengths, J. Meteor., 11, 58–67.

Wentz, F. J. , S. Peteherych, and L. A. Thomas, 1984: A model function for ocean radar cross sections at 14.6 GHz, Journal of Geophysical Research, 89(C3), 3689-3704.